

# Radiative Transfer within an Arbitrary Isotropically Scattering Medium Enclosed by Diffuse Surfaces

Jenn-Der Lin\*

National Chiao Tung University, Hsinchu, Taiwan, Republic of China

The exact integral expressions are presented for radiative transfer in an arbitrary three-dimensional absorbing, emitting, isotropically scattering medium enclosed by diffuse surfaces. This paper also presents a straightforward method, the nodal approximation technique, for solving the numerical results of radiative transfer in a medium of arbitrary geometry. The advantageous properties of the method include geometric generality and easy handling of even discontinuous surface loading and/or material property variations. Two examples of different types of geometries, a one-dimensional concentric cylinder and a two-dimensional rectangular enclosure, are analyzed and compared to the existing results to illustrate the accuracy and applicability of the present method. Results show that the present method can accurately predict the radiation distributions.

## Nomenclature

$a$	= dummy variable
$f, g$	= emission functions
$I(r, r')$	= radiation intensity at the point $r$ in the direction $r'$
$I_r(r)$	= inward intensity at the boundary point $r$
$I_b[T(r)]$	= blackbody radiation intensity
$I_b, S_j$	= nodal parameters
$k$	= absorption coefficient
$K, H$	= kernels
$m, n$	= inward unit vectors normal to boundary
$n$	= refractive index of the medium
$m, p$	= number of parameters $S_j$ and $I_i$ , respectively
$M, N$	= interpolation functions
$q(r)$	= net radiative heat flux vector at $r$
$r$	= position vector
$r$	= radial coordinate
$R_1, R_2$	= inner and outer radii, respectively
$S(r)$	= source function
$T$	= temperature
$V_r, \Gamma_r$	= portions of medium volume and surface, respectively, that can be directly seen by one located at $r$
$x$	= coordinates
$\tau_x, \tau_y$	= optical variables for a two-dimensional rectangular geometry
$\tau_{xo}, \tau_{yo}$	= optical width and thickness of a two-dimensional rectangle, respectively
$\beta$	= extinction coefficient
$\delta$	= Kronecker delta
$\epsilon$	= emissivity
$\nu$	= frequency
$\rho$	= hemispherical reflectivity
$\sigma$	= Stefan-Boltzmann constant
$\sigma_s$	= scattering coefficient
$\Omega$	= solid angle
$\omega$	= albedo

## Introduction

**R**ADIATIVE heat transfer through scattering media has been a problem of considerable interdisciplinary interest. For example, the consideration of scattering and absorption of coal and fly ash is important in the determination of heat transfer within pulverized-fuel-fired furnaces. Scattering of radiation by suspensions of small particles also arises in the nuclear industry, powder and/or fibrous insulations, and meteorology. The consideration of scattering adds to the complexity of the radiative transfer problem. Not much work has been done in the area of multidimensional scattering media.

Crosbie and Linsenbardt presented a literature review of multidimensional radiative transfer in scattering media.<sup>1</sup> Their review showed a lack of exact analyses and numerical results. The exact expressions were presented by Crosbie, Schrenker, and Farrell only for radiative transfer in three-dimensional rectangular and cylindrical geometries.<sup>2,3</sup> Crosbie and Schrenker also solved for radiation distribution in a two-dimensional rectangular medium exposed to diffuse radiation.<sup>4</sup> In these formulations and studies, the reflections on the boundaries were not included.

The extensive review of the literature in Ref. 1 also showed that most of the theoretical work listed used some sort of approximation in their formulation. These approximate methods were often developed for selective cases of radiative heat transport. Turner and Love used the time-consuming Monte Carlo statistical method to solve for the directional emittance from a semi-infinite slab.<sup>5</sup> The same method was also utilized by Taniguchi and Funazu to solve for the temperature distribution in a three-dimensional rectangular furnace.<sup>6</sup> A modified differential approximation was applied by Glatt and Olfe to study a two-dimensional rectangular medium in radiative equilibrium.<sup>7</sup> Modest<sup>8</sup> improved this technique for the same medium, and compared results to Hottel's zonal method.<sup>9</sup> The same medium was also studied by Ratzell and Howell with the use of the  $P-N$  approximation.<sup>10</sup> Yuen and Tien proposed a successive approximation approach for the solution of a two-dimensional problem with planar geometry based on a differential formulation.<sup>11</sup> Fiveland used the discrete-ordinates method to solve for radiation distribution in a two-dimensional rectangular scattering medium.<sup>12</sup>

In this paper, exact expressions are presented for radiative heat transport in an arbitrary emitting, absorbing, and isotropically scattering finite medium. The diffuse reflections on the boundaries are included. The expressions are valid for

Received Nov. 18, 1986; presented as Paper 87-0325 at the AIAA 25th Aerospace Sciences Meeting, Reno, NV, Jan. 12-15, 1987; revision received March 6, 1987. Copyright © American Institute of Aeronautics and Astronautics, Inc., 1987. All rights reserved.

\*Associate Professor, Department of Mechanical Engineering.

convex geometries or concave geometries with no re-entrant radiation. These expressions reduce to the formulations that Hottel and Cohen obtained when they devised the zonal method as a lumped-system approximation and considered a nonscattering medium.<sup>13</sup> In order to find the numerical results of radiative transfer in any medium of regular or even irregular geometry, the nodal approximation technique is utilized.<sup>14</sup> The method reduces to the general radiation/finite-element model. Similar methods had been applied by several investigators to one-dimensional and two-dimensional radiative cases.<sup>15-19</sup> Among those studies, Wu et al.<sup>15</sup> presented a rather more general radiation model than the others, using zone-method results. In this study, the nodal approximation technique allows the replacement of formal integral equations by an equivalent discrete system of algebraic equations for the determination of the nodal parameters. The method is quite straightforward and would result in the solutions in a functional relation. Two examples, one-dimensional cylinders and two-dimensional rectangular media for which the exact numerical results are available, are considered to illustrate the accuracy and applicability of the present method. Results show that the present method can accurately predict the radiation distributions.

### Formulation

We consider an absorbing, emitting, and isotropically scattering medium. The medium is isotropic and is characterized by an absorption coefficient  $k$  and scattering coefficient  $\sigma_s$ . The diffuse reflections on the boundaries are included. Time variable and the subscript  $\nu$ , which denotes the spectrally dependent properties, are omitted for simplicity.

If we assume that a local thermodynamic equilibrium is established and that the Kirchhoff law is valid, the expression for the source function can be written as<sup>20</sup>

$$S(r) = k(r)I_b [T(r)] + \frac{\sigma_s(r)}{4\pi} \left\{ \int_{V_r} \int S(r'') \frac{1}{|r - r''|^2} \times \exp \left\{ - \int_0^1 \beta [r + a(r'' - r)] |r - r''| da \right\} dV'' + \int_{\Gamma_r} I_r(r') \frac{m \cdot (r - r')}{|r - r'|^3} \times \exp \left\{ - \int_0^1 \beta [r + a(r' - r)] |r - r'| da \right\} dA' \right\} \quad (1)$$

where  $\beta(r) = k(r) + \sigma_s(r)$  is the extinction coefficient of the medium at the location  $r$ ,  $I_r(r')$  the inward boundary intensity at  $r'$ ,  $dV''$  the infinitesimal volume about the interior point  $r''$ , and  $dA'$  the infinitesimal area about the boundary point

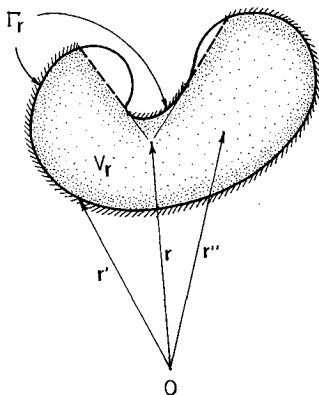


Fig. 1 Illustration of the volume and surface of integration for concave geometries.

$r'$  with inward unit normal  $m$ .  $V_r$  and  $\Gamma_r$  are, respectively, the whole volume and surface for a convex medium. For a concave medium with no re-entrant radiation,  $V_r$  and  $\Gamma_r$  are the portions of medium volume and surface, respectively, that can be directly seen from point  $r$ , as illustrated in Fig. 1.

The net radiant flux vector at location  $r$  is<sup>20</sup>

$$q(r) = \int_{V_r} \int S(r'') \frac{r - r''}{|r - r''|^3} \times \exp \left\{ - \int_0^1 \beta [r + a(r'' - r)] |r - r''| da \right\} dV'' + \int_{\Gamma_r} I_r(r') \frac{r - r'}{|r - r'|^4} [m \cdot (r - r')] \times \exp \left\{ - \int_0^1 \beta [r + a(r' - r)] |r - r'| da \right\} dA' \quad (2)$$

The boundary intensity at point  $r$  with inward unit normal  $n$ , as shown in Fig. 2, is given as

$$I_r(r) = \epsilon(r)I_b [T(r)] + \frac{\rho(r)}{\pi} [q_{in}(r) \cdot (-n)]$$

where  $q_{in}(r)$  is the incident radiant flux on the boundary at  $r$ , and  $\epsilon(r)$  and  $\rho(r)$  are, respectively, the emissivity and hemispherical reflectivity.

Using Eq. (2), the boundary intensity can be written as

$$I_r(r) = \epsilon(r)I_b [T(r)] + \frac{\rho(r)}{\pi} \left\{ \left( \int_{V_r} \int S(r'') \frac{n \cdot (r'' - r)}{|r - r''|^3} \times \exp \left\{ - \int_0^1 \beta [r + a(r'' - r)] |r - r''| da \right\} dV'' + \int_{\Gamma_r} I_r(r') \frac{n \cdot (r' - r)}{|r - r'|^4} [m \cdot (r - r')] \times \exp \left\{ - \int_0^1 \beta [r + a(r' - r)] |r - r'| da \right\} dA' \right) \right\} \quad (3)$$

Both Eqs. (1) and (3) formulate the radiative transfer in an arbitrary medium bounded by diffuse surfaces. Once the source function and boundary distributions are solved, the net radiant flux distributions are readily obtained by Eq. (2).

### Divergence of Radiant Flux Vector and Radiative Equilibrium

The divergence of the net radiant flux vector  $\nabla \cdot q(r)$  characterizes the net radiative energy emitted or absorbed by

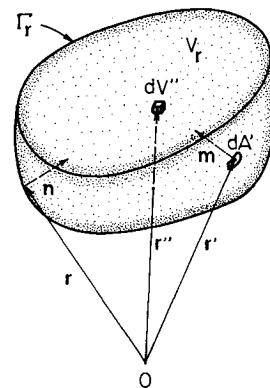


Fig. 2 Coordinate system for boundary intensity for a general three-dimensional geometry.

the matter because of radiation to and from a volume of medium at  $r$ .  $\nabla \cdot \mathbf{q}(r)$  is given by

$$\begin{aligned}\nabla \cdot \mathbf{q}(r) &= 4\pi k(r) I_b[T(r)] - k(r) \int_{4\pi} I(r, \Omega) d\Omega \\ &= \frac{4\pi k(r)}{\sigma_s(r)} \{ \beta(r) I_b[T(r)] - S(r) \}\end{aligned}$$

For a gray medium at radiative equilibrium that is enclosed by diffuse surfaces,

$$\nabla \cdot \mathbf{q}(r) = 0 \text{ and } S(r) = \beta(r) I_b[T(r)] = \beta(r) n^2 \sigma T^4(r) / \pi$$

where  $n$  is the refractive index of the medium.

Equations (1) and (3) then become

$$\begin{aligned}\frac{n^2 \sigma T^4(r)}{\pi} &= \frac{1}{4\pi} \left( \int_{V_r} \int \beta(r'') \frac{n^2 \sigma T^4(r'')}{\pi} \frac{1}{|r - r''|^2} \right. \\ &\times \exp \left\{ - \int_0^1 \beta[r + a(r'' - r)] |r - r''| da \right\} dV'' \\ &+ \int_{\Gamma_r} \int I_{\Gamma}(r') \frac{\mathbf{m} \cdot (\mathbf{r} - \mathbf{r}')}{|\mathbf{r} - \mathbf{r}'|^3} \\ &\times \exp \left\{ - \int_0^1 \beta[r + a(r' - r)] |r - r'| da \right\} dA' \end{aligned} \quad (4)$$

and

$$\begin{aligned}I_{\Gamma}(r) &= \epsilon(r) \frac{n^2 \sigma T^4(r)}{\pi} + \frac{\rho(r)}{\pi} \left( \int_{V_r} \int \beta(r'') \frac{\mathbf{n} \cdot (\mathbf{r}'' - \mathbf{r})}{|\mathbf{r} - \mathbf{r}''|^3} \right. \\ &\times \exp \left\{ - \int_0^1 \beta[r + a(r'' - r)] |r - r''| da \right\} dV'' \\ &+ \int_{\Gamma_r} \int I_{\Gamma}(r') \frac{\mathbf{n} \cdot (\mathbf{r}' - \mathbf{r})}{|\mathbf{r} - \mathbf{r}'|^4} [\mathbf{m} \cdot (\mathbf{r} - \mathbf{r}')] \\ &\times \exp \left\{ - \int_0^1 \beta[r + a(r' - r)] |r - r'| da \right\} dA' \end{aligned} \quad (5)$$

Equations (4) and (5) are coupled integral expressions for the temperature distribution of any gray finite medium at radiative equilibrium.

### Nodal Approximation

Equations (1) and (3) can be written in brief forms as

$$\begin{aligned}S(x) &= f(x) + \frac{\sigma_s(x)}{4\pi} \left\{ \int_{V_x} \int S(x'') K_1(x, x'') dV'' \right. \\ &\left. + \int_{\Gamma_x} \int I_{\Gamma}(x') H_1(x, x') dA' \right\} \end{aligned} \quad (6)$$

and

$$\begin{aligned}I_{\Gamma}(x') &= g(x') + \frac{\rho(x')}{\pi} \left\{ \int_{V_{x'}} \int S(x'') K_2(x', x'') dV'' \right. \\ &\left. + \int_{\Gamma_{x'}} \int I_{\Gamma}(x) H_2(x, x') dA' \right\} \end{aligned} \quad (7)$$

where  $x$  and  $x'$  are coordinates of points. The radiant emission from a volume of the medium at  $x$  and from boundary surface at  $x'$  is represented by  $f(x)$  and  $g(x')$ , respectively. That is,  $f = kn^2 \sigma T^4 / \pi$  and  $g = \epsilon \sigma T^4 / \pi$ . The kernels  $K(x, x')$  and  $H(x, x')$  are influence functions and assign the proper size of influence caused by radiation source at  $x'$  to radiative strength at  $x$ . The kernels are explicitly expressed in Eqs. (1) and (3). Both Eqs. (6) and (7) are

Fredholm-type integral equations when the medium is convex and Volterra-type for concave geometries.

Equations (6) and (7) are coupled owing to the reflection effect on the boundaries. Analytic solutions of source function and boundary intensity are difficult to obtain. To construct approximations  $S(x)$  and  $I_{\Gamma}(x')$ , the nodal approximation technique is utilized over the geometric domain of the medium. Let  $S_{ap}(x)$  be an approximation of  $S(x)$  and  $I_{ap}(x')$  an approximation of  $I_{\Gamma}(x')$ . To construct approximations  $S_{ap}(x)$  and  $I_{ap}(x')$ , it suffices to write expressions

$$S_{ap}(x) = N_1(x) S_1 + N_2(x) S_2 + \cdots + N_m(x) S_m \quad (8)$$

and

$$I_{ap}(x') = M_1(x') I_1 + M_2(x') I_2 + \cdots + M_p(x') I_p \quad (9)$$

where  $S_i = S(x_i)$  and  $I_j = I_{\Gamma}(x'_j)$  are the nodal parameters and  $N_i(x)$  and  $M_j(x')$  are the interpolation functions. The interpolation functions possess the properties

$$N_j(x_i) = \delta_{ij} \quad M_p(x'_q) = \delta_{pq}$$

where  $\delta$  is the Kronecker delta.

Equations (8) and (9) can also be written in matrix form as

$$\begin{aligned}\langle S_{ap}(x) \rangle &= \langle N_1(x), N_2(x), \cdots, N_m(x) \rangle \begin{bmatrix} S_1 \\ S_2 \\ \vdots \\ S_m \end{bmatrix} \\ &= \langle N(x) \rangle [S_m] \end{aligned} \quad (10)$$

and

$$\begin{aligned}\langle I_{ap}(x') \rangle &= \langle M_1(x'), M_2(x'), \cdots, M_p(x') \rangle \begin{bmatrix} I_1 \\ I_2 \\ \vdots \\ I_p \end{bmatrix} \\ &= \langle M(x') \rangle [I_p] \end{aligned} \quad (11)$$

where  $\langle N \rangle$  denotes a single-row matrix and  $[N]$  represents a single-column matrix.

Substitution of Eqs. (10) and (11) into Eqs. (6) and (7) gives

$$\begin{aligned}\langle N(x) \rangle [S_m] &= \langle f(x) \rangle + \langle \sigma_s(x) / 4\pi \rangle \{ \langle N^1(x) \rangle [S_m] \\ &+ \langle M^1(x') \rangle [I_p] \} \end{aligned} \quad (12)$$

for  $x$  in the geometrical domain of the medium, and

$$\begin{aligned}\langle M(x') \rangle [I_p] &= \langle g(x') \rangle + \langle \rho(x') / \pi \rangle \{ \langle N^2(x') \rangle [S_m] \\ &+ \langle M^2(x') \rangle [I_p] \} \end{aligned} \quad (13)$$

for  $x'$  on the medium boundary, where

$$N^i(x) = \int_{V_x} \int N(x'') K_i(x, x'') dV''$$

and

$$M^i(x') = \int_{\Gamma_{x'}} \int M(x'') H_i(x, x') dA'$$

Equations (12) and (13) construct the expressions for approximating functions  $S_{ap}(x)$  and  $I_{ap}(x')$ . Both equations must, of course, hold for all values of  $x$  and  $x'$  and, consequently, in particular for  $x = x_1, x_2, \cdots, x_m$  and  $x' = x'_1, x'_2, \cdots, x'_p$ .

By the procedure just adopted, the original integral Eqs. (1) and (3) have been replaced by a system of  $(m + p)$  approxi-

mate nonhomogeneous linear algebraic equations to solve for the  $(m + p)$  unknowns  $S_1, S_2, \dots, S_m, I_1, I_2, \dots, I_p$ . The solution of these equations by means of ordinary algebraic methods furnishes the values of the unknown functions at  $(m + p)$  points. One can then approximate solutions of source function and boundary intensity by nodal approximation.

The appropriate interpolation functions  $N_i(x)$  and  $M_j(x')$  must be constructed for each domain. A straightforward choice is taking the Lagrange polynomials as interpolation functions. That is,

$$N_i(x) = \prod_{\substack{j=1 \\ j \neq i}}^m (x - x_j)/(x_i - x_j), \quad i = 1, 2, \dots, m$$

and

$$M_j(x') = \prod_{\substack{i=1 \\ i \neq j}}^p (x' - x'_i)/(x'_j - x'_i), \quad j = 1, 2, \dots, p$$

They are utilized in one-dimensional concentric cylinders.

When the shape of the geometric domain of the medium is irregular or the number of nodes increases, more complexity is introduced for the construction of approximating functions  $S_{ap}(x)$  and  $I_{ap}(x')$  over the whole geometric domain of the medium. For such a case, nodal approximations by subdomain, called finite element, would simplify the construction of  $S_{ap}(x)$  and  $I_{ap}(x')$  and could be easily implemented in a computer.

### Sample Examples and Discussion

To illustrate the accuracy and applicability of the present method associated with the formulated exact expressions, two examples are studied: a one-dimensional concentric cylinder and a two-dimensional rectangular geometry, which are, respectively, concave and convex geometries. All the integrals encountered in the numerical computations are performed by 8-point Gaussian quadrature.

#### One-Dimensional Concentric Cylinder

The present work studies the radiative equilibrium temperature distributions in a gray homogeneous medium between two concentric cylinders, as illustrated in Fig. 3. The inner and outer cylinder walls, respectively, have the hemispheric reflectivities  $\rho_1$  and  $\rho_2$ . This problem serves as a good indication on the effectiveness of the present method because

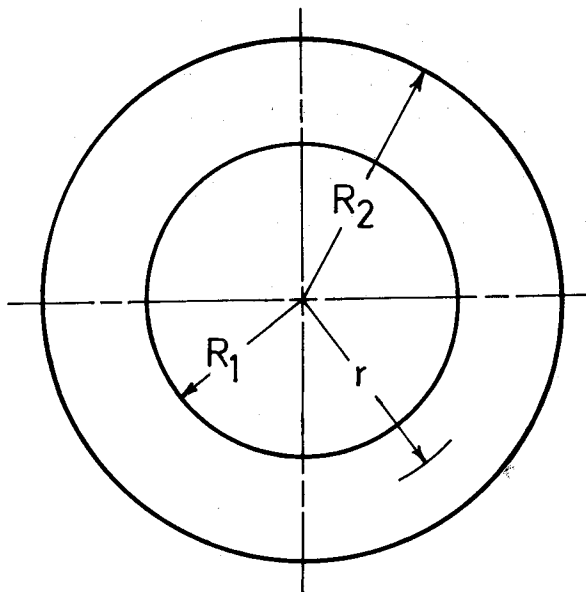


Fig. 3 Schematic diagram of the concentric cylinder.

the Monte Carlo solution at  $\rho_1 = \rho_2 = 0$  is available to check the accuracy of the approximate solution.

The radiative equilibrium temperature for the present system can be obtained from Eqs. (4) and (5). Using the nodal approximation technique, the four-node approximations are obtained. The nodes are chosen to be at  $(r - R_1)/(R_2 - R_1) = 0.01, 0.18, 0.4$ , and  $0.75$ . Figures 4 and 5 show the comparison of radiative equilibrium temperature with Monte Carlo solution<sup>21</sup> and modified differential approximation<sup>22</sup> for media with  $R_2/R_1 = 10$  and  $\epsilon_1 = \epsilon_2 = 1$  at two values of optical thickness  $(R_2 - R_1)$ . Present results are in better agreement with statistical Monte Carlo solution than modified differential approximation. The present work also examines the effect of surface reflectivities on the emissive power distribution, as illustrated in Table 1. Since the emissivity is for many surfaces

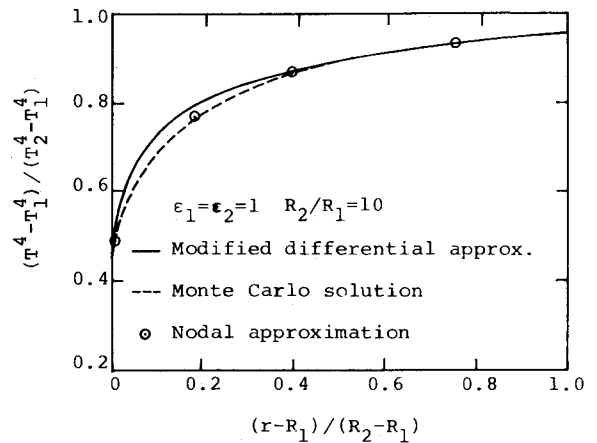


Fig. 4 Comparison of radiative equilibrium temperature distribution in a concentric cylinder at  $R_2 - R_1 = 2$ .

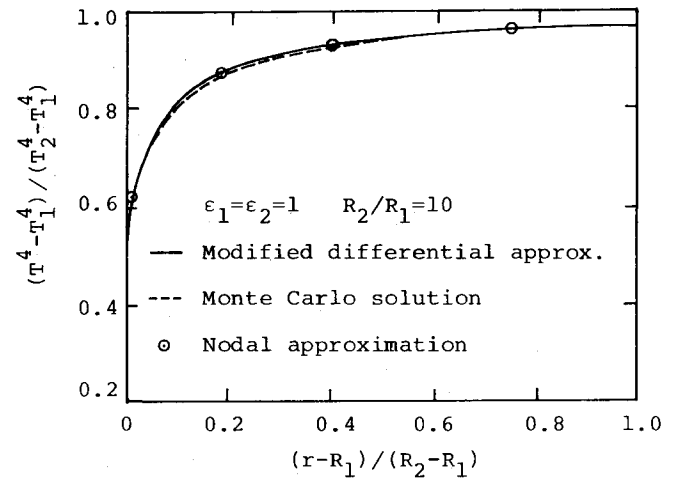


Fig. 5 Comparison of radiative equilibrium temperature distribution in a concentric cylinder at  $R_2 - R_1 = 0.1$ .

Table 1 Radiative equilibrium temperature,  $[\sigma T^4/\pi - I_r(R_2)]/[I_r(R_1) - I_r(R_2)]$ , at nodal points under various surface conditions ( $R_2/R_1 = 1.5$ ,  $R_2 - R_1 = 0.1$ )

Locations	$\rho_1 = 0$	$\rho_1 = 0.1$	$\rho_1 = 0.1$	$\rho_1 = 0.2$	$\rho_1 = 0.2$
	$\rho_2 = 0$	$\rho_2 = 0.1$	$\rho_2 = 0.2$	$\rho_2 = 0.1$	$\rho_2 = 0.2$
$\frac{r - R_1}{R_2 - R_1} = 0.01$	0.509	0.509	0.510	0.510	0.510
0.18	0.400	0.400	0.400	0.400	0.400
0.40	0.335	0.335	0.335	0.335	0.335
0.75	0.267	0.267	0.267	0.267	0.267

above 0.8, results are thus for the surface reflectivity of 0, 0.1, and 0.2. It is observed that the surface conditions do not affect the dimensionless emissive power,  $[\sigma T^4/\pi - I_T(R_2)]/I_T(R_1) - I_T(R_2)$ , although the boundary intensities vary with surface conditions. The intensity at the hot surface decreases with the increase in surface reflectivity at a given temperature. The intensity at the cold surface increases with the surface reflectivity.

### Two-Dimensional Rectangular Problem

To illustrate the effectiveness of the present method for multidimensional radiative transfer, a two-dimensional rectangular homogeneous medium exposed to radiation is considered. The same medium has been studied by several investigators.<sup>4,10,12,18</sup> Figure 6 illustrates the coordinate system and the geometry being studied. For the present system, the formal integral expression, Eq. (1), for the source function is solved.

The construction of approximating functions  $S(\tau_x, \tau_y)$  gets more complicated and difficult when the number of nodes increases. The whole domain of the rectangle is thus subdivided into subrectangles, and approximations with finite elements are considered. Linear approximations over each element are utilized. Figure 7 shows the  $6 \times 6$  nodal approximation of the dimensionless source function  $S/I_T(\tau_x, 0)$  for rectangular geometries in radiative equilibrium with only uniform diffuse radiation incident on the top surface and  $\epsilon_1 = \epsilon_2 = \epsilon_3 = \epsilon_4 = 1$  at  $2\tau_{x0} = \tau_{y0} = 1$ . Present results show a good agreement with the existing solutions. The effect of absorption, or single scattering albedo on the dimensionless source function  $S[\omega I_T(\tau_x, 0)]$ , is presented for a nonemitting

medium with only uniform diffuse radiation incident on the top surface. Tables 2 and 3 show the comparison with Crosbie and Schrenker's results<sup>4</sup> for albedo equal to 0.9 and 0.5 at  $2\tau_{x0} = \tau_{y0} = 1$ . Results are in excellent agreement except at points  $(\pm \tau_{x0}, 0)$ . Crosbie and Schrenker's results show unstable answers at both points and the present results agree with their higher values of results at these points.

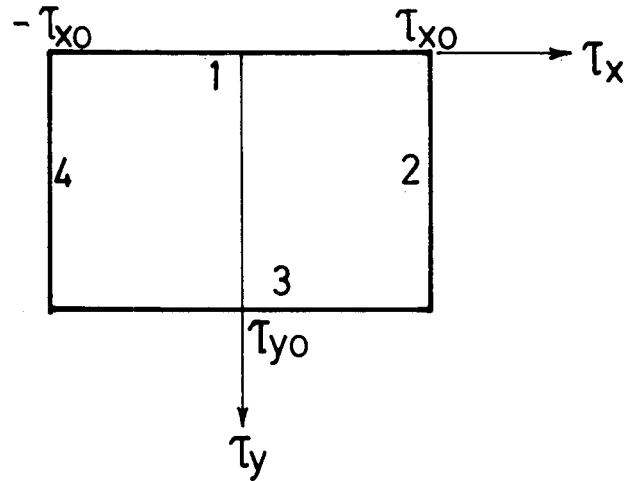


Fig. 6 Schematic of rectangular geometry.

Table 2 Comparison of the source function,  $S/[\omega I_T(\tau_x, 0)]$ , with results for a medium exposed to a diffuse strip,  $2\tau_{x0} = \tau_{y0} = 1$  and  $\omega = 0.9$ .

$\frac{\tau_x}{\tau_{x0}}$	Top		Bottom		$\frac{\tau_y}{\tau_{y0}}$	Side		Center	
	Ref. 4	Present study	Ref. 4	Present study		Ref. 4	Present study	Ref. 4	Present study
0	0.6102	0.6116	0.0776	0.0781	0	0.3064	0.5578	0.6102	0.6116
0.12796	0.6097		0.0772		0.07216	0.2607		0.5208	
0.2		0.6104		0.0771	0.1		0.2482		0.4943
0.25381	0.6080		0.0760		0.10884	0.2440		0.4844	
0.37550	0.6052		0.0742		0.15194	0.2268		0.4452	
0.4		0.6063		0.0742	0.2		0.2102		0.4070
0.49102	0.6013		0.0718		0.20076	0.2093		0.4048	
0.59848	0.5966		0.0690		0.37309	0.1595		0.2896	
0.6		0.5981		0.0694	0.4		0.1537		0.2767
0.69612	0.5910		0.0661		0.43602	0.1446		0.2566	
0.78232	0.5848		0.0631		0.68775	0.0969		0.1585	
0.8		0.5843		0.0628	0.7		0.0955		0.1561
0.85566	0.5782		0.0603		0.74551	0.0880		0.1416	
1.0	0.5564	0.5578	0.0536	0.0539	1.0	0.0536	0.0539	0.0776	0.0781

Table 3 Comparison of the source function,  $S/[\omega I_T(\tau_x, 0)]$ , with results for a medium exposed to a diffuse strip,  $2\tau_{x0} = \tau_{y0} = 1$  and  $\omega = 0.5$ .

$\frac{\tau_x}{\tau_{x0}}$	Top		Bottom		$\frac{\tau_y}{\tau_{y0}}$	Side		Center	
	Ref. 4	Present study	Ref. 4	Present study		Ref. 4	Present study	Ref. 4	Present study
0	0.5510	0.5522	0.0543	0.0547	0	0.2761	0.5277	0.5510	0.5522
0.12796	0.5508		0.0540		0.07216	0.2241		0.4431	
0.2		0.5516		0.0541	0.1		0.2115		0.4139
0.25381	0.5501		0.0533		0.10884	0.2064		0.4037	
0.37550	0.5489		0.0521		0.15194	0.1885		0.3632	
0.4		0.5497		0.0522	0.2		0.1720		0.3247
0.49102	0.5472		0.0506		0.20076	0.1710		0.3231	
0.59848	0.5451		0.0489		0.37309	0.1240		0.2164	
0.6		0.5461		0.0492	0.4		0.1187		0.2048
0.69612	0.5426		0.0470		0.43602	0.1107		0.1878	
0.78232	0.5397		0.0452		0.68775	0.0709		0.1090	
0.8		0.5402		0.0451	0.7		0.0699		0.1071
0.85566	0.5367		0.0435		0.74551	0.0640		0.0965	
1.0	0.5261	0.5277	0.0396	0.0399	1.0	0.0396	0.0399	0.0543	0.0547

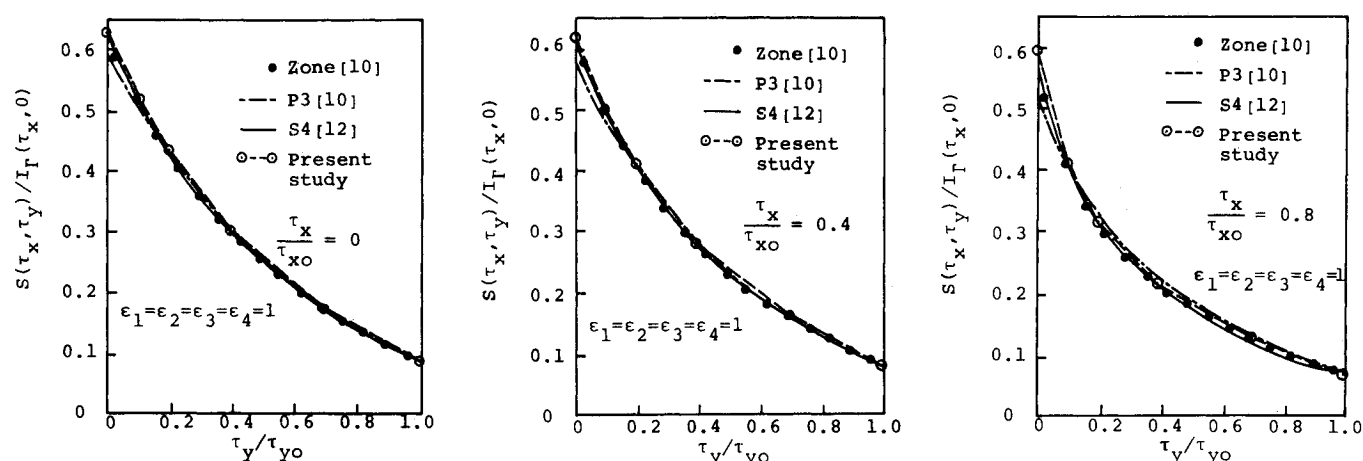


Fig. 7 Source function of rectangular geometries in radiative equilibrium at  $2\tau_{x0} = \tau_{y0} = 1$ .

### Conclusions

The formal integral equations describing radiative transfer in an arbitrary isotropically scattering medium enclosed by diffuse surfaces were developed. The nodal approximation technique was then applied to these equations. The technique allowed the replacement of the integral equations by a system of algebraic equations for the determination of nodal values. A property of the interpolation functions used is that the approximation error vanishes at all nodal points. When the shape of the geometric domain of the medium is irregular or the number of nodes increases, the construction of the interpolation Eqs. (10) and (11) could be simplified with the nodal approximations by finite elements. This reduces to the general radiation/finite-element model. To model a problem of such cases, we decide on the number, type, and shape of elements. Each of these factors may contribute to the so-called discretization error. Geometric discretization error is associated with modeling a curved boundary by straight-sided elements. It is easy to reduce by either increasing the number of elements or using curved boundaries.<sup>14</sup> It must also be noted that the arrangement of a given number of elements influences results most strongly if the mesh is coarse. Nevertheless, the finite-element method will converge toward the correct answer as the element size is decreased, i.e., the number of nodes is increased, provided that the interpolation equations give constant values throughout the element when the nodal values are numerically identical.<sup>23</sup>

Two examples of different types of geometries were considered in the paper. Numerical results were in excellent agreement with the existing solutions. Because the present study is concerned only with isotropic scattering and diffuse surfaces, it is recommended that the exact expressions be developed next for anisotropic scattering with nondiffuse reflection on the boundary and that the applicability of the present method to such problems be studied.

### References

- <sup>1</sup>Crosbie, A.L. and Linsenhardt, T.L., "Two-Dimensional Isotropic Scattering in a Semi-Infinite Medium," *Journal of Quantitative Spectroscopy and Radiative Transfer*, Vol. 19, No. 3, 1978, pp. 257-284.
- <sup>2</sup>Crosbie, A.L. and Schrenker, R.G., "Exact Expressions for Radiative Transfer in a Three-Dimensional Rectangular Geometry," *Journal of Quantitative Spectroscopy and Radiative Transfer*, Vol. 28, No. 6, 1982, pp. 507-526.
- <sup>3</sup>Crosbie, A.L. and Farrell, J.B., "Exact Formulation of Multiple Scattering in a 3-D Cylindrical Geometry," *Journal of Quantitative Spectroscopy and Radiative Transfer*, Vol. 31, No. 5, 1984, pp. 397-416.
- <sup>4</sup>Crosbie, A.L. and Schrenker, R.G., "Radiative Transfer in a Two-Dimensional Rectangular Medium Exposed to Diffuse Radiation," *Journal of Quantitative Spectroscopy and Radiative Transfer*, Vol. 31, No. 4, 1984, pp. 339-372.
- <sup>5</sup>Turner, W.D. and Love, T.J., "Directional Emittance of a Two-Dimensional Ceramic Coating," *AIAA Journal*, Vol. 9, Sept. 1971, pp. 1849-1853.
- <sup>6</sup>Taniguchi, H. and Funazu, M., "The Numerical Analysis of Temperature Distributions in a Three-Dimensional Furnace," *Bulletin of JSME*, Vol. 13, Dec. 1970, pp. 1458-1468.
- <sup>7</sup>Glatt, L. and Olfe, D.B., "Radiative Equilibrium of a Gray Medium in a Rectangular Enclosure," *Journal of Quantitative Spectroscopy and Radiative Transfer*, Vol. 13, No. 9, 1973, pp. 881-895.
- <sup>8</sup>Modest, M.F., "Radiative Equilibrium in a Rectangular Enclosure Bounded by Gray Walls," *Journal of Quantitative Spectroscopy and Radiative Transfer*, Vol. 15, No. 6, 1975, pp. 445-461.
- <sup>9</sup>Hottel, H.C. and Sarofim, A.F., *Radiative Transfer*, McGraw-Hill, New York, 1967.
- <sup>10</sup>Ratzel, A.C. and Howell, J.R., "Two-Dimensional Radiation in Absorbing-Emitting Media Using the P-N Approximation," *Journal of Heat Transfer*, Vol. 105, No. 2, 1983, pp. 333-340.
- <sup>11</sup>Yuen, W.W. and Tien, C.L., "Successive Approximation Approach to Problems in Radiative Transfer with a Differential Formulation," *Journal of Heat Transfer*, Vol. 102, 1980, pp. 86-91.
- <sup>12</sup>Fiveland, W.A., "Discrete-Ordinates Solutions of the Radiative Transport Equation for Rectangular Enclosures," *Journal of Heat Transfer*, Vol. 106, No. 4, 1984, pp. 699-706.
- <sup>13</sup>Hottel, H.C. and Cohen, E.S., "Radiant Heat Exchange in a Gas-Filled Enclosure: Allowance for Nonuniformity of Gas Temperature," *AIChE Journal*, Vol. 4, No. 1, 1958, pp. 3-14.
- <sup>14</sup>Dhatt, G. and Touzot, G., *The Finite Element Method Displayed*, Wiley, New York, 1984.
- <sup>15</sup>Wu, S.T., Ferguson, R.E., and Altgilbers, L.L., "Application of Finite Element Techniques to Interaction of Conduction and Radiation in Participating Medium," *Progress in Astronautics and Aeronautics: Heat Transfer and Thermal Control*, Vol. 78, AIAA, New York, 1980, pp. 61-91.
- <sup>16</sup>Fernandes, R.L., Francis, J.E., and Reddy, J.N., "A Finite-Element Approach to Combined Conductive and Radiative Heat Transfer in a Planar Medium," *Progress in Astronautics and Aeronautics: Heat Transfer and Thermal Control*, Vol. 78, AIAA, New York, 1980, pp. 92-109.
- <sup>17</sup>Fernandes, R.L. and Francis, J.E., "Combined Radiative and Conductive Heat Transfer in a Planar Medium with a Flux Boundary Condition Using Finite Elements," *AIAA Paper 82-0910*, June 1982.
- <sup>18</sup>Razzaque, M.M., Klein, D.E., and Howell, J.R., "Finite Element Solution of Radiative Heat Transfer in a Two-Dimensional Rectangular Enclosure with Gray Participating Media," *Journal of Heat*

*Transfer*, Vol. 105, 1983, pp. 933-936.

<sup>19</sup>Razzaque, M.M., Howell, J.R., and Klein, D.E., "Coupled Radiative and Conductive Heat Transfer in a Two-Dimensional Enclosure with Gray Participating Media Using Finite Element," *Proceedings of the ASME/JSME Thermal Engineering Joint Conference*, Honolulu, March 1983, Vol. 4, pp. 41-47, also *Journal of Heat Transfer*, Vol. 106, No. 3, 1984, pp. 613-619.

<sup>20</sup>Lin, J.D., "Exact Expressions for Radiative Transfer in an Arbitrary Geometry Exposed to Radiation," *Journal of Quantitative Spectroscopy and Radiative Transfer*, Vol. 37, No. 6, 1987, pp.

591-601.

<sup>21</sup>Perlmutter, M. and Howell, J.R., "Radiant Transfer Through a Gray Gas Between Concentric Cylinders Using Monte Carlo," *Journal of Heat Transfer*, Vol. 86, No. 2, 1964, pp. 169-179.

<sup>22</sup>Olfe, D.B., "Application of a Modified Differential Approximation to Radiative Transfer in a Gray Medium Between Concentric Spheres and Cylinders," *Journal of Quantitative Spectroscopy and Radiative Transfer*, Vol. 8, No. 3, 1968, pp. 899-907.

<sup>23</sup>Segerlind, L.J., *Applied Finite Element Analysis*, Wiley, New York, 1976.

## *From the AIAA Progress in Astronautics and Aeronautics Series*

### **THERMOPHYSICS OF ATMOSPHERIC ENTRY—v. 82**

*Edited by T.E. Horton, The University of Mississippi*

Thermophysics denotes a blend of the classical sciences of heat transfer, fluid mechanics, materials, and electromagnetic theory with the microphysical sciences of solid state, physical optics, and atomic and molecular dynamics. All of these sciences are involved and interconnected in the problem of entry into a planetary atmosphere at spaceflight speeds. At such high speeds, the adjacent atmospheric gas is not only compressed and heated to very high temperatures, but strongly reactive, highly radiative, and electronically conductive as well. At the same time, as a consequence of the intense surface heating, the temperature of the material of the entry vehicle is raised to a degree such that material ablation and chemical reaction become prominent. This volume deals with all of these processes, as they are viewed by the research and engineering community today, not only at the detailed physical and chemical level, but also at the system engineering and design level, for spacecraft intended for entry into the atmosphere of the earth and those of other planets. The twenty-two papers in this volume represent some of the most important recent advances in this field, contributed by highly qualified research scientists and engineers with intimate knowledge of current problems.

*Published in 1982, 521 pp., 6×9, illus., \$29.95 Mem., \$59.95 List*

TO ORDER WRITE: Publications Dept., AIAA, 370 L'Enfant Promenade S.W., Washington, D.C. 20024-2518